Advanced Research Center for Beam Science – Electron Microscopy and Crystal Chemistry –

http://eels.kuicr.kyoto-u.ac.jp/EMCC/home-en.html

Prof
KURATA, Hiroki
(D Sc)

Assoc Prof
HARUTA, Mitsutaka
(D Sc)

Assist Prof
NEMOTO, Takashi
(D Sc)

Program-Specific Res*
KIYOMURA, Tsutomu

*Nanotechnology Platform

Researchers (pt)

OGAWA, Tetsuya (D Sc)
YAMAGUCHI, Atsushi (D Sc)

Students

IWASHIMIZU, Chisaki (D3)
LIN, I-Ching (D2)
KAZAMA, Hiroki (M2)
SATO, Shinya (M1)
MORIMOTO, Syunji (M1)
YASUI, Kentaro (M1)

Scope of Research

We study crystallographic and electronic structures of materials and their transformations through direct imaging of atoms or molecules by high-resolution electron spectromicroscopy, which realizes energy-filtered imaging and electron energy-loss spectroscopy as well as high-resolution imaging. By combining this with scanning probe microscopy, we cover the following subjects: 1) direct structure analysis, electron crystallographic analysis, 2) elemental analysis and electronic states analysis, 3) structure formation in solutions, and 4) epitaxial growth of molecules.

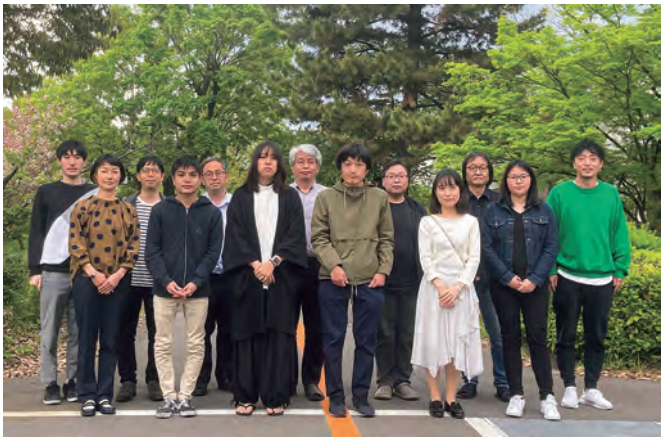

KEYWORDS

STEM-EELS ELNES Spectrum Imaging Electron Orbital Multiple Frame Acqusition

Recent Selected Publications

Haruta, M.; Kikkawa, J.; Kimoto, K.; Kurata, H., Comparison of Detection Limits of Direct-Counting CMOS and CCD Cameras in EELS Experiments, *Ultramicroscopy*, **240,** [113577-1]-[113577-6] (2022).

Haruta, M.; Nemoto, T.; Kurata, H., Sub-picometer Sensitivity and Effect of Anisotropic Atomic Vibrations on Ti $L_{2,3}$-Edge Spectrum of $SrTiO_3$, *Appl. Phys. Lett.*, **119,** [232901-1]-[232901-5] (2021).

Iwashimizu, C.; Haruta, M.; Kurata, H., Electron Orbital Mapping of $SrTiO_3$ Using Electron Energy-Loss Spectroscopy, *Appl. Phys. Lett.*, **119,** [232902-1]-[232902-5] (2021).

Haruta, M.; Nii, A.; Hosaka, Y.; Ichikawa, N.; Saito, T.; Shimakawa, Y.; Kurata, H., Extraction of the Local Coordination and Electronic Structures of FeO_6 Octahedra Using Crystal Field Multiplet Calculations Combined with STEM-EELS, *Appl. Phys. Lett.*, **117,** [132902-1]-[132902-5] (2020).

Yamaguchi, A.; Nemoto, T.; Kurata, H., Study of C K-Edge High Energy Resolution Energy-Loss Near-Edge Structures of Copper Phthalocyanine and Its Chlorinated Molecular Crystals by First-Principles Band Structure Calculations, *J. Phys. Chem. A*, **124,** 1735-1743 (2020).

Electron Orbital Mapping of $SrTiO_3$ Using Electron Energy-Loss Spectroscopy (EELS)

The visualization of electron orbitals in real space is expected as a next-generation technique that has been evolved from high spatial resolution electron microscopy. Although its possibility has recently theoretically reported by using an energy-filtered energy-loss near-edge structure (ELNES) mapping, the experimental demonstration has been quite challenging because of the low signal-to-noise ratio (SNR). Here, we present the visualization of 2*p* electron orbitals of oxygen in $SrTiO_3$ in real space using STEM-EELS combined with newly developed our multi-frame acquisition approach that dramatically improves the SNR.

The experiment was carried out using a spherical aberration corrected STEM (JEOL; JEM-ARM200F) with an EELS spectrometer (Gatan; GIF Quantum ERS). Spectrum imaging (SI) data of about 100 × 1000 pixels were obtained. Image distortion due to sample drift was suppressed as much as possible by measuring the SI data in a horizontally narrow scan area with a short acquisition time of 2ms per pixel. Individual SI data was applied the subtraction of ultra-high-quality dark reference spectrum obtained from the average of 20 000 dark spectra and then the original gain-correction. To improve the SNR of the spectrum and to correct the image distortion, 7762 SI data were summed using the multi-frame non-rigid registration combined with a template matching technique. Spectral deconvolution by zero-loss peak was applied to improve the energy resolution. In the present experiment, in order to minimize sample drift and obtain high signal intensity, we prioritized the acquisition of SI data in a short time using a high-current incident probe rather than the acquisition of high-energy resolution spectra. Finally, weighted-principal component analysis (W-PCA) was used to remove spectral noise.

Figure 1(b) shows the oxygen *p*-partial density of states (PDOS) of unoccupied bands at the O1 site and simulated O K-ELNES. Figure 1(c) shows the experimental O K-ELNES. It is suggested that peaks a and d are mainly composed of a single component of $p_{x,y}$ (hybridized with Ti 3*d*(t_{2g}) forming a π*-bond), while peaks b and e are composed of p_z (hybridized with Ti 3*d*(e_g) forming a σ*-bond) orbitals. Figures 2(a) and 2(b) show ground state charge density maps projected along the [110] axis for the unoccupied states of π*- and σ*-bonds, respectively. The distribution at oxygen sites is anisotropic, which reflects the orientation of the 2*p* orbitals. In the oxygen map in Fig. 2(d), oxygen atoms were not observed in the Sr-O columns because the atomic density of oxygen is half compared to the pure oxygen columns. Figures 2(e)–2(h) show O K-ELNES maps using the intensities of peaks a, b, d, and e. Figures 2(e) and 2(g) show vertically elongated ellipses, while Figs. 2(f) and 2(h) show lateral ellipses. These orientations agree well with those of the calculated charge density distribution showing oxygen *p*-orbitals. In summary, we experimentally demonstrated the visualization of 2*p* electron orbitals of oxygen in the $SrTiO_3$ [110] projection in real space. Although orbital mapping has been a challenge due to the SNR problem with spectra, improvement of the SNR for a core-loss spectrum measured with atomic resolution has made it possible to observe electron orbitals using electron microscopy.

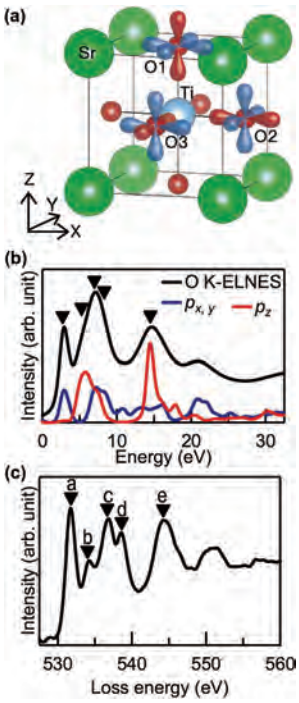

Figure 1. PDOS and oxygen K-ELNES of $SrTiO_3$. (a) Structural model of $SrTiO_3$. The O 2*p* orbitals can be classified into two groups: the blue orbitals distributed in the Sr–O plane, hybridized with the Ti 3*d* orbitals with t_{2g} symmetry, and the red orbitals distributed in the direction of the Ti–O–Ti bond, hybridized with Ti 3*d* orbitals with e_g symmetry. (b) Simulated O K-ELNES (black) and oxygen *p* PDOS for O1 sites (blue and red). (c) Experimental O K-ELNES.

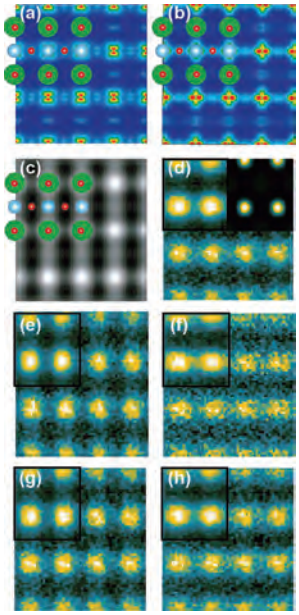

Figure 2. Projection along the [110] axis. Charge density maps for the unoccupied state of the (a) π*-bond (3–4 eV) and (b) σ*-bond (5–6 eV). (c) Accumulated HAADF image along the [110] axis. (d) Oxygen elemental map using an energy window of 26 eV from the threshold of the O K-edge. O-ELNES mappings using (e) peak a, (f) peak b, (g) peak d, and (h) peak e. The upper left insets in (d)–(h) are the results of W-PCA. The upper right inset in (d) is a simulated elemental mapping.